Author(s): Dodds, Stephen J.
Article title: Hyper Sliding Mode Control: A Novel Approach Achieving Robustness With Model Order Uncertainty
Year of publication: 2006
Citation: Dodds, S.J. (2006) 'Hyper Sliding Mode Control: A Novel Approach Achieving Robustness With Model Order Uncertainty' Proceedings of the AC&T, pp.142-148.
Link to published version:
http://www.uel.ac.uk/act/proceedings/documents/ACT06Proceeding.pdf

HYPER SLIDING MODE CONTROL: A NOVEL APPROACH ACHIEVING ROBUSTNESS WITH MODEL ORDER UNCERTAINTY

Stephen J Dodds
Control Research Group
stephen.dodds@spacecon.co.uk; s.j.dodds@uel.ac.uk

Abstract: A novel approach to the control of plants with model order uncertainty as well as parametric errors and external disturbances is presented, which yields a specified closed loop dynamic response. Its foundations lie in sliding mode control, but the set of output derivatives fed back extend to a maximum order of $r_{max} - 1$, where r_{max} is the maximum likely rank of the plant. In conventional sliding mode control, the number of output derivatives fed back is a set of state variables equal in number to $r - 1$, where r is the rank of the plant and derivatives of higher order than $r - 1$, which are not state variables, are not fed back, meaning that the plant order must be known in advance. In hyper sliding mode control, originated by the author, although the output derivatives of higher order than r are not plant state variables, *they become state variables of the closed-loop system* and *take part in the sliding mode.* Thus, in cases where the maximum order of the output derivative exceeds $r - 1$, the order of the closed-loop system is greater than that of the plant, which is a small price to pay for retaining the extreme robustness properties of sliding mode control.
The method is illustrated by means of simulations of a motion control system employing a permanent magnet synchronous motor. An initial evaluation of the method is made by considering three plants with different orders and ranks, the first being the unloaded drive, the second being the drive controlling the motor rotor angle with a mass-spring load attached and the third being the drive controlling the load mass angle of the same attached mass-spring load. The simulations indicate that the control system does indeed yield robustness including plant order uncertainty.

1. Introduction

Sliding mode control (Utkin, 1992) is a well known technique for achieving robustness, but only with respect to external disturbances and uncertainties in the parameters of a plant model of known form. This method, as it stands, cannot achieve robustness with respect to plant model order uncertainty but when the model order is known, it not only achieves stability but can achieve a specified closed-loop dynamic response that does not change significantly in the presence of parametric changes or external disturbances. It is also applicable to nonlinear plants. This paper presents an approach that retains the robustness features of conventional sliding mode control and additionally accommodates plant order uncertainty.
The method was discovered as a result of an experiment on sliding mode control that worked successfully despite an error that violated the conventional rules of control theory. In order to describe this situation, the sliding mode control method will be briefly described. Figure 1 shows the general block diagram of a sliding mode control system designed to yield a precisely defined closed-loop dynamic performance for a single input, single output (SISO) plant.

There are many different forms of sliding mode control system, but this one will suffice for the purpose of this paper.

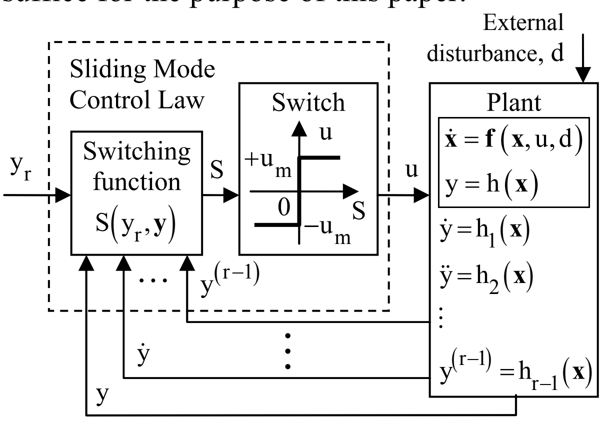

Figure 1: General SISO sliding mode control.

Here, $\mathbf{x} = \left[x_1\, x_2 \cdots x_n\right]^T$, is the state vector, where n is the order of the plant, and $\mathbf{y} = \left[y\,\dot{y} \cdots y^{(r-1)}\right]^T$ is the vector of output derivatives. The rank (or relative degree) of the plant is r, such that the r^th^ output derivative is $y^{(r)} = h_r(\mathbf{x}, u)$ and is *not* a state variable because of its dependence on the control input, u. The elements of y are *all state variables* and the set of equations for the derivatives of y constitute a transformation to a new set of state variables. As can be seen, the sliding mode control law is a bang-bang control law in which u switches between maximum and minimum values of $\pm u_m$ when S passes through zero. The switching surface, $S(y_r, \mathbf{y}) = 0$, is designed such that over the normal range of operating states, u is automatically switched to the value that drives y towards the surface. In this way, y is held on the surface while u rapidly switches between $+u_m$ and $-u_m$, in theory at an infinite frequency and with a continuously varying mark-space ratio. Under these circumstances, the point, y, in the output derivative space appears to *slide* in the surface and the system is said to be operating in a *sliding mode*. Also, during this *sliding motion*, the closed-loop system is governed by the differential equation, $S(y_r, \mathbf{y}) = 0$, i.e.,

$$S\left(y_r, y\,\dot{y} \cdots y^{(r-1)}\right) = 0. \qquad (1)$$

Remarkably, if the switching function, is linear, i.e.,

$$S(y_r, \mathbf{y}) = y_r - \left(y + q_1\dot{y} + q_2\ddot{y} + \ldots + q_{r-1}y^{(r-1)}\right)$$

then the closed loop system is linear with transfer function

$$\frac{y(s)}{y_r(s)} = \frac{1}{1 + sq_1 + s^2q_2 + \ldots + s^{r-1}q_{r-1}} \qquad (2)$$

which is *independent of the plant parameters and the external disturbance*. Furthermore, the coefficients, q_1, q_2, …, q_{r-1}, may be chosen independently to design the system by pole assignment to achieve *any desired dynamic performance*, within the limitations of the hardware. It must also be realised that this performance is only attained while in sliding motion. The condition for sliding motion is that the point, y, in the r dimensional space with components, $y_r, y, \dot{y}, \cdots y^{(r-1)}$, is driven back towards the switching surface (1) from both sides by the control law. This is expressed mathematically as

$$S\dot{S} < 0 \qquad (3)$$

This condition will only be satisfied over a finite region of the switching surface and, in general, this region may be increased in size by increasing the maximum control level, u_m.

The sliding mode control system described above is a state feedback control system. If the plant is of full rank, then $r = n$ and $\mathbf{y} = \left[y\,\dot{y} \cdots y^{(n-1)}\right]^T$ is a complete state vector, enabling complete control of the plant according to standard control theory. If, however, the plant is not of full rank, i.e., $r < n$, then the sliding mode control law can only control a subsystem of the plant with the state variables, $y_r, y, \dot{y}, \cdots y^{(r-1)}$. There then exists an uncontrolled subsystem of order, $n - r$. The dynamics of this uncontrolled subsystem is referred to as the *zero dynamics.* In fact, a linear plant with transfer function, $y(s)/u(s) = N(s)/D(s)$, which is not of full rank has $n - r$ zeros and the poles characterising the zero dynamics are roots of $N(s) = 0$, i.e., the plant *zeros*. Zero dynamics will be seen in one of the plants considered later.

2. Output Derivative Feedback Robust Control Law

According to standard control theory, it is only necessary to feed back a complete set of state variables to the control law. In particular, attempting to feed back variables such as $y^{(r)} = h_r(\mathbf{x}, u)$ or higher derivatives of y is really considered 'against the rules' because of the creation of algebraic loops through their dependence on u and its derivatives. The proposed control law, however, deliberately uses these further derivatives and is simply that of Figure 1 without any restriction on the order of the output derivatives being fed back and with the switch replaced by the gain, K. In this case, $S(y_r, \mathbf{y})$ will be called simply the *sliding function* since there is no switch. It is shown in Figure 3 for a linear plant and a linear sliding function.

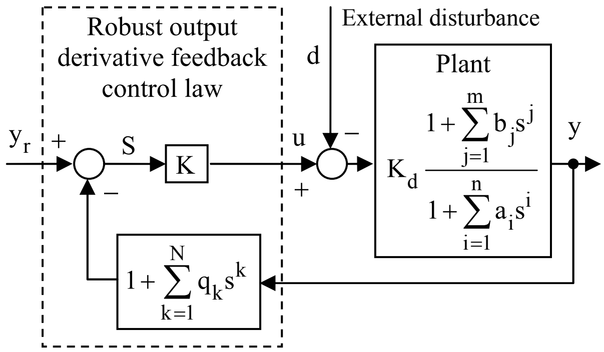

Figure 3: Linear output derivative robust control law applied to a linear plant.

Then

$$y(s) = \frac{K_d\left(1+\sum_{j=1}^{m} b_j s^j\right)\left[y_r(s) - \frac{1}{K}d(s)\right]}{\frac{1}{K}\left(1+\sum_{i=1}^{n} a_i s^i\right) + K_d\left(1+\sum_{k=1}^{N} q_k s^k\right)\left(1+\sum_{j=1}^{m} b_j s^j\right)}$$

Thus the order, of the closed-loop system is

$$n_c = \begin{cases} n & \text{if } N+m \le n \\ N+m & \text{if } N+m > n \end{cases} \tag{4}$$

If $N + m > n$, then the following applies:

$$\lim_{K \to \infty} y(s) = \frac{1}{1+\sum_{k=1}^{N} q_k s^k} . y_r(s) \tag{5}$$

The system can then be designed by pole assignment but in the above limit, the closed loop characteristic equation becomes:

$$\left(1+\sum_{k=1}^{N} q_k s^k\right)\left(1+\sum_{j=1}^{m} b_j s^j\right) = 0 \tag{6}$$

and therefore m of the closed-loop poles are the zeros of the plant transfer function, which cannot be changed and it is essential that all of these poles are in the left half of the s-plane. It is evident that the order of the closed-loop system increases beyond the plant order, n, by an amount equal to the number of output derivatives that do not qualify as state variables. If plant model order uncertainty is considered, it is necessary to choose an upper limit, r_{max}, of the plant rank, which the real plant is guaranteed not to exceed. Then the controller can be designed with $N = r_{max}$. *In fact, the controller will produce the same closed-loop performance, according to* (5)*, for a whole range of different plants of rank ranging between* 1 *and* r_{max}.

3. Application to a Vector Controlled PMSM Drive

In this section a motion control system will be developed for a simulation study of hyper sliding mode control. The plant is a vector controlled PMSM driving a mechanical load of variable order and rank. First the mechanism will be described and modelled. Then a practicable version of the robust output derivative control law will be formulated. Figure 4 shows an overall block diagram of the motion control system.

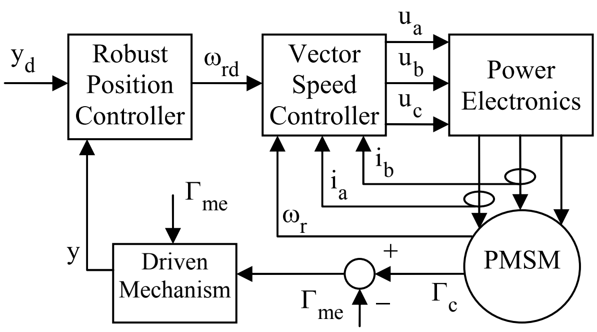

Figure 4: Motion control system for simulation study

3.1 Driven mechanism

The driven mechanism is a balanced mass with moment of inertia, J_L, coupled to the motor shaft via a torsion spring with spring constant, K_s, as shown in Figure 5.

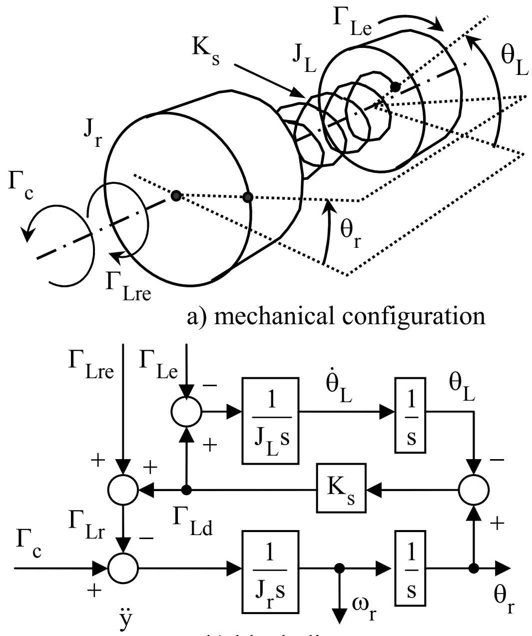

Figure 5: Model of the driven mechanism.

The corresponding torque balance equations are as follows:

$$J_r \ddot{\theta}_r = \Gamma_c - \Gamma_{Lre} + K_s\left(\theta_L - \theta_r\right) \tag{7a}$$

$$J_L \ddot{\theta}_L = K_s\left(\theta_r - \theta_L\right) - \Gamma_{Le} \tag{7b}$$

where J_r is the rotor moment of inertia, θ_r is the rotor angle, θ_L is the load mass angle, Γ_{Lre} and Γ_{Le} are the external load torques applied, respectively, to the rotor and the load mass and Γ_c is the control torque produced by the motor.

The vector control scheme is based on forced dynamic control (Dodds, 2005), yielding the following speed control loop transfer function:

$$\frac{\omega_r(s)}{\omega_{rd}(s)} = \left(\frac{1}{1 + \left(9/2T_{s\omega}\right)s}\right)^2 \tag{8}$$

From Figure 5, the transfer function relationships with $\omega_r(s)$ as input, for plants

1, 2 are both $\frac{\theta_r(s)}{\omega_r(s)}=\frac{1}{s}$ and for plant 3 is $\theta_L(s)=\frac{K_s\omega_r(s)-s\Gamma_{Le}(s)}{s\left(J_L s^2+K_s\right)}$. Combining these with (8) yields the following plants:

Plants 1 and 2:

$$\frac{\theta_r(s)}{\omega_{rd}(s)}=\frac{1}{s}\left(\frac{1}{1+\left(9/2T_{s\omega}\right)s}\right)^2 \tag{9}$$

Plant 3:

$$\theta_L(s)=\frac{K_s\omega_{rd}(s)-s\left(1+\frac{9}{2T_{s\omega}}s\right)^2\Gamma_{Le}(s)}{s\left(1+\frac{9}{2T_{s\omega}}s\right)^2\left(J_L s^2+K_s\right)} \tag{10}$$

The fact that Plants 1 and 2 are identical and independent of the rotor external load torque, Γ_{Lre}, is due to the robustness already given by the forced dynamic speed control law (Dodds, 2005) which artificially decouples the mass-spring load from the system.
With reference to (9) and (10), the maximum rank is $r_{max}=5$. Figure 7 shows a block diagram of the outer robust position control loop for this case corresponding to Figure 3, with low-pass measurement noise filtering, with a time constant, $T_f \ll T_s$ where T_s is the settling time. It is assumed that, as is usual in electrical drives the angular velocity measurements, ω_r and $\dot{\theta}_L$, are both available, so that only three approximate differentiations are necessary in the controller. The output derivative feedback gains, q_1 to q_4 are determined by pole assignment, using the author's settling time formula, $T_s=1.5(1+N)T_c$, for a linear system with coincident poles at $s=-1/T_c$.

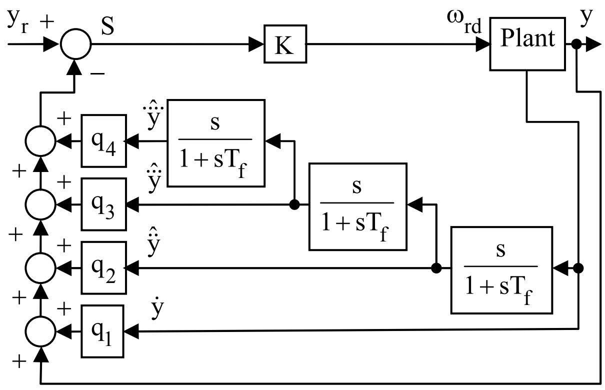

Figure 7: Outer robust control loop

In this case

$$\frac{y(s)}{y_r(s)}=\frac{1}{1+q_1s+q_2s^2+\ldots q_Ns^N}=\frac{1}{\left(1+s\frac{T_s}{1.5(1+N)}\right)^N}$$

where $N=r_{max}-1=4$.

Thus:

$$\begin{cases} q_1=4.\left(2T_s/15\right) & q_2=6.\left(2T_s/15\right)^2 \\ q_3=4.\left(2T_s/15\right)^3 & q_4=\left(2T_s/15\right)^4 \end{cases} \tag{11}$$

4. Simulations

The Mechanical load parameters for plants 2 and 3 are: JL=0.01 Kgm^2; Ks=9 Nm/rad
The forced dynamic control law parameters are set to T_s = 0.2s; K=200; T_f = 0.0001s; T_{so} = 0.001s; with the derivative feedback gains according to (22).
For all three plants, a step reference angle of 2 rad was applied. The robustness against external disturbances was tested by applying external load torques according to Figure 7.

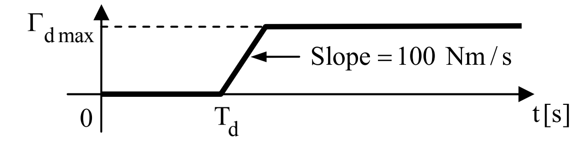

	Plant 1	Plants 2 and 3
Γ_{Lre} [Nm]	$\Gamma_{d\max} = 3$ N $T_d = 0.5\,s$	$\Gamma_{d\max} = 3$ Nm $T_d = 0.5\,s$
Γ_{Le} [Nm]	Not applicable	$\Gamma_{d\max} = 1\,Nm$

Figure 7: External load torques.

Figures 8 to 15 show simulations without mismatching of the PMSM parameters.
It is evident from Figure 8 that the system is very robust with respect to changes in the driven mechanical load and both load torques.

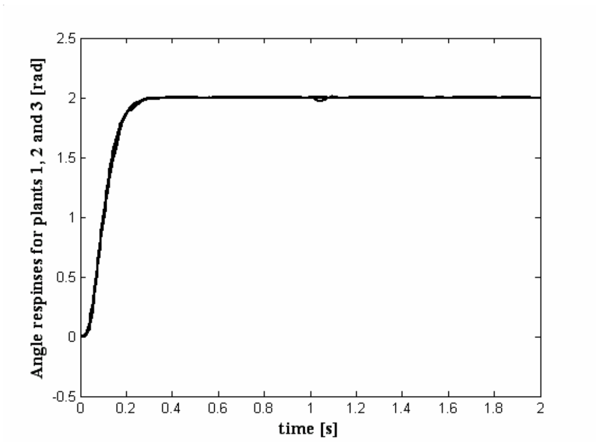

Figure 8: Angle step responses of Plants 1, 2 and 3.

Figure 12 shows the rotor angle for Plant 2 being very accurately controlled while the sprung load mass is uncontrolled and left to oscillate. This is a consequence of the dynamic load torque, Γ_d, being counteracted by the forced dynamic inner loop speed controller (Dodds 2005).

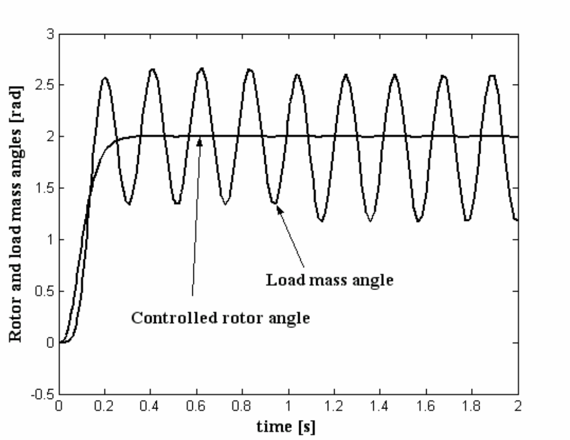

Figure 12: Plant 2 rotor and load mass angles.

Further development of the robust controller would be needed in order to achieve active damping of the sprung load mass oscillations while satisfactorily controlling the rotor angle. Figure 14 shows the sprung load mass angle being accurately controlled while the rotor angle is varied by the controller to apply the necessary control torques to the sprung mass via the spring.

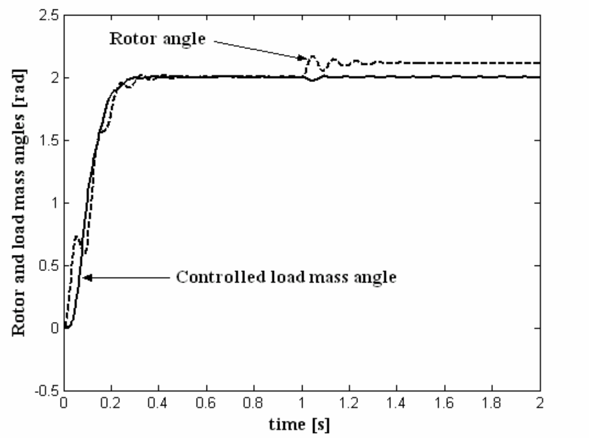

Figure 14: Plant 3 rotor and load mass angles.

In contrast to Plant 2, Plant 3 is of full rank (no transfer function zeros) and this explains the stable behaviour of the whole system. Figure 16 shows the responses of all three plants when the rotor moment of inertia is over-estimated by 50%.

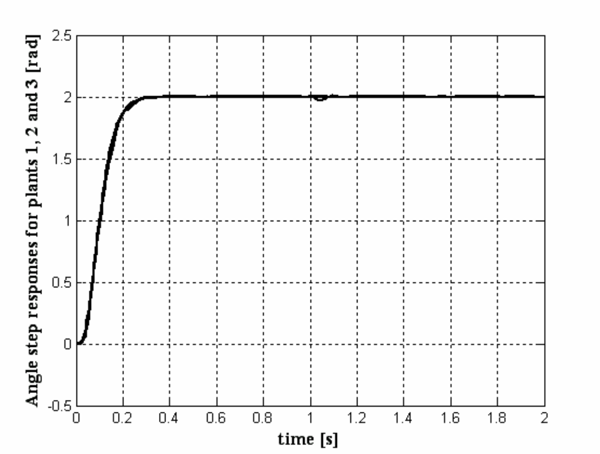

Figure 16: Responses: +50% rotor m.o.i. error.

The remarkable degree of robustness is achieved by the forced dynamic controller, since such an error in the rotor moment of inertia is equivalent to an added (or subtracted) rotor mass, reflected by a change in the dynamic load torque, Γ_{Ld}, (ref., Figure 5), which is estimated by the observer and counteracted by the controller (Dodds 2005).

5. Conclusions and Suggestions for Further Work

The simulations carried out indicate that the new robust output derivative controller is capable of controlling the selected third and fifth order plants with the same specified dynamic responses, in the presence of external disturbances. It is therefore recommended that the technique is investigated for a much wider range of plants.

5. References

Dodds, S. J., "A Novel Approach To Robust Motion Control Of Electrical Drives With Model Order Uncertainty", *6th International Conference Elektro 2005,* Zilina, Slovakia.

Utkin, V. I., Sliding Modes in Control and Optimisation, Springer Verlag, 1992.